The energy sources on the right-hand side of Eq. (5) are the same as that appearing in the energy balance Eq. (1) and, except for T_D, their efficiency factors can be expressed using the parameters characterizing the reference state of the core. It can then be proved that all terms, except the radioactive heating one, is a function of the radius of the inner core and is proportional to its growth rate. This means that, if the heat flow across the CMB is known, this growth rate can be computed from the energy equation (1), and the entropy equation (5) then gives the ohmic dissipation that is maintained. Alternatively, one can take the opposite view and compute the growth rate of the inner core that is required to maintain a given ohmic dissipation, the energy balance being then used to get the heat flow across the CMB that makes this growth rate happen. Unfortunately, the ohmic dissipation in the core is no better known than the heat flow across the CMB, since it is dominated by small-scales of the magnetic field and possibly by the invisible toroidal part of it (Gubbins and Roberts, 1987; Roberts *et al*., 2003). However, the value of $Q_{\mathrm{CMB}} = 10$ TW used above gives a contribution of ohmic dissipation to the entropy balance $\mathbf{\Phi}/T_{\mathrm{D}} = 500\ \mathrm{MWK}^{-1}$. The temperature T_{D} is not well-known, but is bounded by the temperature at the inner core boundary and the CMB and this gives $\mathbf{\Phi} \simeq 2$ TW.

The evolution with time of the entropy balance associated with a given heat flow evolution can be computed and the example shown above gives the result of Figure G12. An interesting feature is the sharp increase of the ohmic dissipation in the core when the inner core starts crystallizing, latent heat and, even more so, gravitational energy being more efficient than secular cooling. Unfortunately, the link between this ohmic dissipation and the magnetic field observed at the surface of the Earth is far from obvious and the detection of such an increase in the paleomagnetic record is unlikely (Labrosse and Macouin, 2003).

Some alternative models for the average structure of the core involving some stratification have been proposed. In particular, the heat conducted along the adiabatic temperature gradient can be rather large (about 7 TW) and might be larger than the heat flow across the CMB (see *Core–mantle boundary, heat flow across*). In this case, two different models have been proposed. In the first one, the adiabatic temperature profile is maintained by compositional convection against thermal stratification, except in a still very thin boundary layer, and this means that the entropy flow across the CMB is less than that required to maintain the conduction along the average temperature profile. In other words, the compositional convection has to fight against thermal stratification to maintain the adiabatic temperature profile in addition to maintaining the dynamo. In the second model (see Labrosse *et al*., (1997); Lister and Buffett (1998)), a subadiabatic layer of several hundreds of kilometers is allowed to develop at the top of the core and the entropy flow out of the core balances the conduction along the average temperature gradient. In this case, the compositional energy is entirely used for the dynamo. Which of these two options would be chosen by the core is a dynamical question that cannot be addressed by simple thermodynamic arguments as used here.

Stéphane Labrosse

Bibliography

Braginsky, S.I., and Roberts, P.H., 1995. Equations governing convection in Earth's core and the geodynamo. *Geophysical Astrophysical Fluid Dynamics*, **79**: 1–97.

Gessmann, C.K., and Wood, B.J., 2002. Potassium in the Earth's core? *Earth and Planetary Science Letters*, **200**: 63–78.

Gubbins, D., and Roberts, P.H., 1987. Magnetohydrodynamics of the Earth's core. In Jacobs, J.A., (ed.), *Geomagnetism*, Vol. 2. London: Academic Press, pp. 1–183.

Labrosse, S., 2003. Thermal and magnetic evolution of the Earth's core. *Physics of the Earth and Planetary Interiors*, **140**: 127–143.

Labrosse, S., and Macouin, M., 2003. The inner core and the geodynamo. *Comptes Rendus Geosciences*, **335**: 37–50.

Labrosse, S., Poirier, J.-P., and Le Mouël, J.-L., 1997. On cooling of the Earth's core. *Physics of the Earth and Planetary Interiors*, **99**: 1–17.

Labrosse, S., Poirier, J.-P., and Le Mouël, J.-L., 2001. The age of the inner core. *Earth and Planetary Science Letters*, **190**: 111–123.

Lee, K.K.M., and Jeanloz, R., 2003. High-pressure alloying of potassium and iron: radioactivity in the Earth's core? *Geophysical Research Letters*, **30**: 2212, doi:10.1029/2003GL018515.

Lister, J.R., and Buffett, B.A., 1995. The strength and efficiency of the thermal and compositional convection in the geodynamo. *Physics of the Earth and Planetary Interiors*, **91**: 17–30.

Lister, J.R., and Buffett, B.A., 1998. Stratification of the outer core at the core–mantle boundary. *Physics of the Earth and Planetary Interiors*, **105**: 5–19.

Poirier, J.-P., 1994. Light elements in the Earth's core: a critical review. *Physics of the Earth and Planetary Interiors*, **85**: 319–337.

Rama Murthy, V., van Westrenen, W., and Fei, Y., 2003. Radioactive heat sources in planetary cores: experimental evidence for potassium. *Nature*, **423**: 163–165.

Roberts, P.H., Jones, C.A., and Calderwood, A.R., 2003. Energy fluxes and ohmic dissipation in the Earth's core. In Jones, C A., Soward, A.M., and Zhang, K. (eds.) *Earth's Core and Lower Mantle.* London: Taylor & Francis, pp. 100–129.

Stevenson, D.J., 1990. Fluid dynamics of core formation. In Newsom, H.E., and Jones, J.H. (eds.) *Origin of the Earth.* New York: Oxford University Press, pp. 231–249.

Cross-references

Convection, Chemical
Core Composition
Core Density
Core Properties, Physical
Core Properties, Theoretical Determination
Core Temperature
Core, Adiabatic Gradient
Core, Boundary Layers
Core–Mantle Boundary, Heat Flow Across
Grüneisen's Parameter for Iron and Earth's Core
Melting Temperature of Iron in the Core, Experimental
Melting Temperature of Iron in the Core, Theory

GEODYNAMO: NUMERICAL SIMULATIONS

Introduction

The *geodynamo* is the name given to the mechanism in the Earth's core that maintains the Earth's magnetic field (see *Geodynamo*). The current consensus is that flow of the liquid iron alloy within the outer core, driven by buoyancy forces and influenced by the Earth's rotation, generates large electric currents that induce magnetic field, compensating for the natural decay of the field. The details of how this produces a slowly changing magnetic field that is mainly dipolar in structure at the Earth's surface, with occasional dipole reversals, has been the subject of considerable research by many people for many years.

The fundamental theory, put forward in the 1950s, is that differential rotation within the fluid core shears poloidal (north–south and radial) magnetic field lines into toroidal (east–west) magnetic field; and three-dimensional (3D) helical fluid flow twists toroidal field lines into poloidal field. The more sheared and twisted the field structure the faster it decays away; that is, magnetic diffusion (reconnection) continually smooths out the field. The field is self-sustaining if, on average, the generation of field is balanced by its decay. Discovering and understanding the details of how rotating convection in Earth's fluid outer

core maintains the observed intensity, structure, and time dependencies requires 3D computer models of the geodynamo.

Magnetohydrodynamic (MHD) dynamo simulations are numerical solutions of a coupled set of nonlinear differential equations that describe the 3D evolution of the thermodynamic variables, the fluid velocity, and the magnetic field. Because so little can be detected about the geodynamo, other than the poloidal magnetic field at the surface (today's field in detail and the paleomagnetic field in much less detail) and what can be inferred from seismic measurements and variations in the length of the day and possibly in the gravitational field, models of the geodynamo are used as much to predict what has not been observed as they are used to explain what has. When such a model generates a magnetic field that, at the model's surface, looks qualitatively similar to the Earth's surface field in terms of structure, intensity, and time-dependence, then it is plausible that the 3D flows and fields inside the model core are qualitatively similar to those in the Earth's core. Analyzing this detailed simulated data provides a physical description and explanation of the model's dynamo mechanism and, by assumption, of the geodynamo.

The first 3D global convective dynamo simulations were developed in the 1980s to study the *solar* dynamo. Gilman and Miller (1981) pioneered this style of research by constructing the first 3D MHD dynamo model. However, they simplified the problem by specifying a constant background density, i.e., they used the Boussinesq approximation of the equations of motion. Glatzmaier (1984) developed a 3D MHD dynamo model using the anelastic approximation, which accounts for the stratification of density within the sun. Zhang and Busse (1988) used a 3D model to study the onset of dynamo action within the Boussinesq approximation. However, the first MHD models of the *Earth's* dynamo that successfully produced a time-dependent and dominantly dipolar field at the model's surface were not published until 1995 (Glatzmaier and Roberts, 1995; Jones *et al*., 1995; Kageyama *et al*., 1995). Since then, several groups around the world have developed dynamo models and several others are currently being designed. Some features of the various simulated fields are robust, like the dominance of the dipolar part of the field outside the core. Other features, like the 3D structure and time-dependence of the temperature, flow, and field inside the core, depend on the chosen boundary conditions, parameter space, and numerical resolution. Many review articles have been written that describe and compare these models (e.g., Hollerbach, 1996; Glatzmaier and Roberts, 1997; Fearn, 1998; Busse, 2000; Dormy *et al*., 2000; Roberts and Glatzmaier, 2000; Christensen *et al*., 2001; Busse, 2002; Glatzmaier, 2002; Kono and Roberts, 2002).

Model description

Models are based on equations that describe fluid dynamics and magnetic field generation. The equation of mass conservation is used with the very good assumption that the fluid flow velocity in the Earth's outer core is small relative to the local sound speed. The anelastic version of mass conservation accounts for a depth-dependent background density; the density at the bottom of the Earth's fluid core is about 20% greater than that at the top. The Boussinesq approximation simplifies the equations further by neglecting this density stratification, i.e., by assuming a constant background density. An equation of state relates perturbations in temperature and pressure to density perturbations, which are used to compute the buoyancy forces, which drive convection. Newton's second law of motion (conservation of momentum) determines how the local fluid velocity changes with time due to buoyancy, pressure gradient, viscous, rotational (Coriolis), and magnetic (Lorentz) forces. The MHD equations (i.e., Maxwell's equations and Ohm's law with the extremely good assumption that the fluid velocity is small relative to the speed of light) describe how the local magnetic field changes with time due to induction by the flow and diffusion due to finite conductivity. The second law of thermodynamics dictates how thermal diffusion and Joule and viscous heating determine the local time rate of change of entropy (or temperature). Additional equations are sometimes included that account for perturbations in composition and gravitational potential and their effects on buoyancy.

This set of coupled nonlinear differential equations, with a set of prescribed boundary conditions, is solved each numerical time step to obtain the evolution in 3D of the fluid flow, magnetic field, and thermodynamic perturbations. Most geodynamo models have employed spherical harmonic expansions in the horizontal directions and either Chebyshev polynomial expansions or finite differences in radius. The equations are integrated in time typically by treating the linear terms implicitly and the nonlinear terms explicitly. The review articles mentioned above describe the variations on the equations, boundary conditions, and numerical methods employed in the various models of the geodynamo.

Current results

Since the mid-1990s, 3D computer simulations have advanced our understanding of the geodynamo. The simulations show that a dominantly dipolar magnetic field, not unlike the Earth's, can be maintained by convection driven by an Earth-like heat flux. A typical snapshot of the simulated magnetic field from a geodynamo model is illustrated in Figure G13 with a set of field lines. In the fluid outer core, where the field is generated, field lines are twisted and sheared by the flow. The field that extends beyond the core is significantly weaker and dominantly dipolar at the model's surface, not unlike the geomagnetic field. For most geodynamo simulations, the nondipolar part of the surface field, at certain locations and times, propagates westward at about $0.2^\circ\ y^{-1}$ as has been observed in the geomagnetic field over the past couple hundred years.

Several dynamo models have electrically conducting inner cores that on average drift eastward relative to the mantle (e.g., Glatzmaier and Roberts, 1995; Sakuraba and Kono, 1999; Christensen *et al*., 2001), opposite to the propagation direction of the surface magnetic

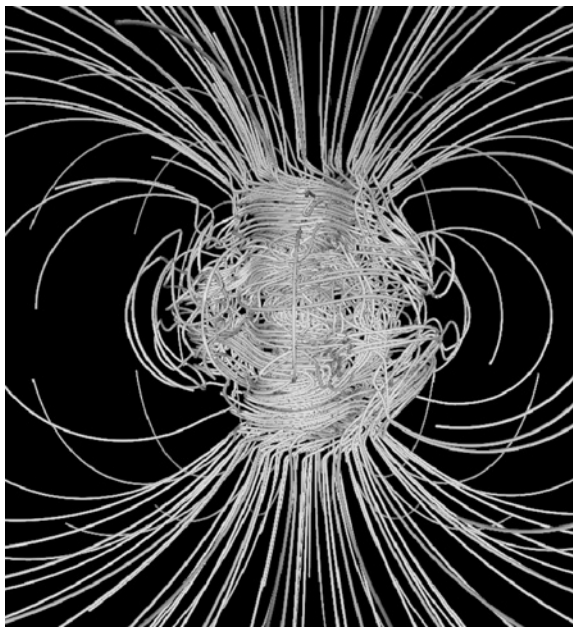

Figure G13 A snapshot of the 3D magnetic field simulated with the Glatzmaier–Roberts geodynamo model and illustrated with a set of magnetic field lines. The axis of rotation is vertical and centered in the image. The field is complicated and intense inside the fluid core where it is generated by the flow; outside the core it is a smooth, dipole-dominated, potential field. (From Glatzmaier, 2002.)

field. Inside the fluid core the simulated flow has a "thermal wind" component that, near the inner core, is predominantly eastward relative to the mantle. Magnetic field in these models that permeates both this flow and the inner core tries to drag the inner core in the direction of the flow. This magnetic torque is resisted by a gravitational torque between the mantle and the topography on the inner core surface. The amplitude of the superrotation rate predicted by geodynamo models depends on the model's prescribed parameters and assumptions and on the very poorly constrained viscosity assumed for the inner core's deformable surface layer, which by definition, is near the melting temperature. The original prediction was an average of about 2° longitude per year faster than the surface. Since then, the superrotation rate of the Earth's inner core (today) has been inferred from several seismic analyzes, but is still controversial. There is a spread in the inferred values, from the initial estimates of 1° to 3° eastward per year (relative to the Earth's surface) to some that are zero to within an uncertainty of 0.2° per year. More recent geodynamo models that include an inhibiting gravitational torque also predict smaller superrotation rates.

On a much longer timescale, the dipolar part of the Earth's field occasionally reverses (see *Reversals, theory*). The reversals seen in the paleomagnetic record are nonperiodic. The times between reversals are measured in hundreds of thousands of years; whereas the time to complete a reversal is typically a few thousand years, less than a magnetic dipole decay time. Several dynamo simulations have produced spontaneous nonperiodic magnetic dipole reversals (Glatzmaier and Roberts, 1995; Glatzmaier *et al*., 1999; Kageyama *et al*., 1999; Sarson and Jones, 1999; Kutzner and Christensen, 2002). Regular (periodic) reversals, like the *dynamo-wave* reversals seen in early solar dynamo simulations, have also occurred in recent dynamo simulations.

One of the simulated reversals is portrayed in Figure G14/Plate 16 with four snapshots spanning about 9 ka. The radial component of the field is shown at both the core–mantle boundary (CMB) and the surface of the model Earth. The reversal, as viewed in these surfaces, begins with reversed magnetic flux patches in both the northern and southern hemispheres. The longitudinally averaged poloidal and toroidal parts of the field inside the core are also illustrated at these times. Although when viewed at the model's surface, the reversal appears complete by the third snapshot, another 3 ka is required for the original field polarity to decay out of the inner core and the new polarity to diffuse in.

Small changes in the local flow structure continually occur in this highly nonlinear chaotic system. These can generate local magnetic anomalies that are reversed relative to the direction of the global dipolar field structure. If the thermal and compositional perturbations continue to drive the fluid flow in a way that amplifies this reversed field polarity while destroying the original polarity, the entire global field structure would eventually reverse. However, more often, the local reversed polarity is not able to survive and the original polarity fully recovers because it takes a couple of thousand years for the original polarity to decay out of the solid inner core. This is a plausible explanation for "events," which occur when the paleomagnetic field (as measured at the Earth's surface) reverses and then reverses back, all within about 10 ka.

On an even longer timescale, the frequency of reversals seen in the paleomagnetic record varies. The frequency of nonperiodic reversals in geodynamo simulations has been found to depend on the pattern of outward heat flux imposed over the CMB (presumably controlled in the Earth by mantle convection) and on the magnitude of the convective driving relative to the effect of rotation.

Many studies have been conducted via dynamo simulations to, for example, assess the effects of the size and conductivity of the solid inner core, of a stably stratified layer at the top of the core, of

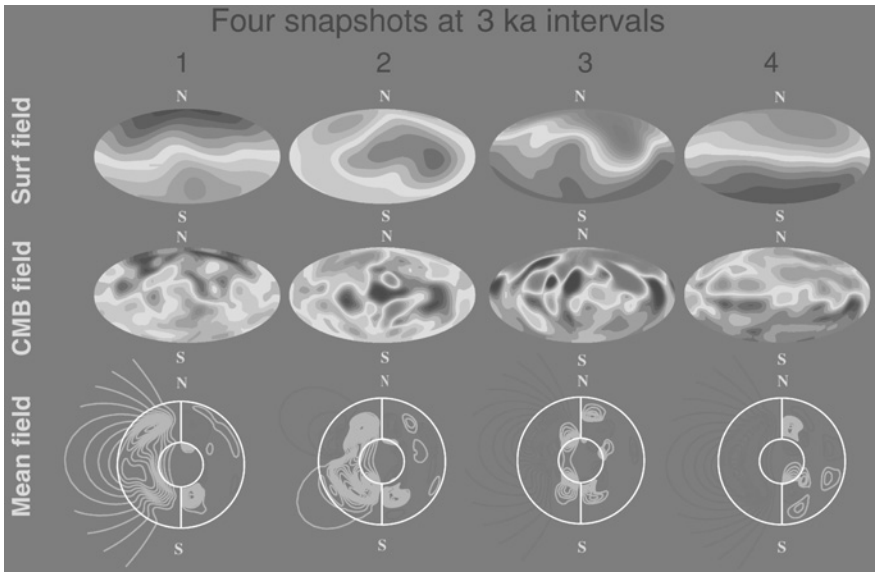

Figure G14/Plate 16 A sequence of snapshots of the longitudinally averaged magnetic field through the interior of the core and of the radial component of the field at the core–mantle boundary and at what would be the surface of the Earth, displayed at roughly 3 ka intervals spanning a dipole reversal from a geodynamo simulation. In the plots of the average field, the small circle represents the inner core boundary and the large circle is the core–mantle boundary. The poloidal field is shown as magnetic field lines on the left-hand sides of these plots (blue is clockwise and red is counterclockwise). The toroidal field direction and intensity are represented as contours (not magnetic field lines) on the right-hand sides (red is eastward and blue is westward). Aitoff–Hammer projections of the entire core–mantle boundary and surface are used to display the radial component of the field (with the two different surfaces displayed as the same size). Reds represent outward directed field and blues represent inward field; the surface field, which is typically an order of magnitude weaker, was multiplied by 10 to enhance the color contrast. (From Glatzmaier *et al*., 1999.)

heterogeneous thermal boundary conditions, of different velocity boundary conditions, and of computing with different parameters. These models differ in several respects. For example, the Boussinesq instead of the anelastic approximation may be used, compositional buoyancy and perturbations in the gravitational field may be neglected, different boundary conditions, and spatial resolutions may be chosen, the inner core may be treated as an insulator instead of a conductor or may not be free to rotate. As a result, the simulated flow and field structures inside the core differ among the various simulations. For example, the strength of the shear flow on the "tangent cylinder" (the imaginary cylinder tangent to the inner core equator; Figure G13), which depends on the relative dominance of the Coriolis forces, is not the same for all simulations. Likewise, the vigor of the convection and the resulting magnetic field generation tends to be greater outside this tangent cylinder for some models and inside for others. But all the solutions have a westward zonal flow in the upper part of the fluid core and a dominantly dipolar magnetic field outside the core.

When assuming Earth values for the radius and rotation rate of the core, all models of the geodynamo have been forced (due to computational limitations) to use a viscous diffusivity that is at least three to four orders of magnitude larger than estimates of what a turbulent (or eddy) viscosity should be (about 2 m^2s^{-1}) for the spatial resolutions that have been employed. In addition to this enhanced viscosity, one must decide how to prescribe the thermal, compositional, and magnetic diffusivities. One of two extremes has typically been chosen. These diffusivities could be set equal to the Earth's actual magnetic diffusivity (2 m^2s^{-1}), making these much smaller than the specified viscous diffusivity; this was the choice for most of the Glatzmaier–Roberts simulations. Alternatively, they could be set equal to the enhanced viscous diffusivity, making all (turbulent) diffusivities too large, but at least equal; this was the choice of most of the other models. Neither choice is satisfactory.

Future challenges

Because of the large turbulent diffusion coefficients, all geodynamo simulations have produced large-scale *laminar* convection. That is, convective cells and plumes of the simulated flow typically span the entire depth of the fluid outer core, unlike the small-scale turbulence that likely exists in the Earth's core.

The fundamental question about geodynamo models is how well do they simulate the actual dynamo mechanism of the Earth's core? Some geodynamo modelers have argued, or at least suggested, that the large (global) scales of the temperature, flow, and field seen in these simulations should be fairly realistic because the prescribed viscous and thermal diffusivities may be asymptotically small enough. For example, in most simulations, viscous forces (away from the boundaries) tend to be 10^4 times smaller than Coriolis and Lorentz forces. Other modelers are less confident that current simulations are realistic even at the large-scales because the model diffusivities are so large. Only when computing resources improve to the point where we can further reduce the turbulent diffusivities by several orders of magnitude and produce strongly turbulent simulations will we be able to answer this fundamental question.

In the mean time, we may be able to get some insight from very highly resolved 2D simulations of magnetoconvection. These simulations can use diffusivities a thousand times smaller than those of the current 3D simulations. They demonstrate that strongly turbulent 2D rotating magnetoconvection has significantly different spatial structure and time-dependence than the corresponding 2D laminar simulations obtained with much larger diffusivities.

These findings suggest that current 3D laminar dynamo simulations may be missing critical dynamical phenomena. Therefore, it is important to strive for much greater spatial resolution in 3D models in order to significantly reduce the enhanced diffusion coefficients and actually simulate turbulence. This will require faster parallel computers and improved numerical methods and hopefully will happen within the next decade or two. In addition, subgrid scale models need to be added to geodynamo models to better represent the heterogeneous anisotropic transport of heat, composition, momentum, and possibly also magnetic field by the part of the turbulence spectrum that remains unresolved.

Gary A. Glatzmaier

Bibliography

Busse, F.H., 2000. Homogeneous dynamos in planetary cores and in the laboratory. *Annual Review of Fluid Mechanics*, **32**: 383–408.

Busse, F.H., 2002. Convective flows in rapidly rotating spheres and their dynamo action. *Physics of Fluids*, **14**: 1301–1314.

Christensen, U.R., Aubert, J., Cardin, P., Dormy, E., Gibbons, S. *et al.,* 2001. A numerical dynamo benchmark. *Physics of the Earth and Planetary Interiors*, **128**: 5–34.

Dormy, E., Valet, J.-P., and Courtillot, V., 2000. Numerical models of the geodynamo and observational constraints. *Geochemistry, Geophysics, Geosystems*, **1**: 1–42, paper 2000GC000062.

Fearn, D.R., 1998. Hydromagnetic flow in planetary cores. *Reports on Progress in Physics*, **61**: 175–235.

Gilman, P.A., and Miller, J., 1981. Dynamically consistent nonlinear dynamos driven by convection in a rotating spherical shell. *Astrophysical Journal, Supplement Series*, **46**: 211–238.

Glatzmaier, G.A., 1984. Numerical simulations of stellar convective dynamos. I. The model and the method. *Journal of Computational Physics*, **55**: 461–484.

Glatzmaier, G.A., 2002. Geodynamo simulations—how realistic are they? *Annual Review of Earth and Planetary Sciences*, **30**: 237–257.

Glatzmaier, G.A., and Roberts, P.H., 1995. A three-dimensional self-consistent computer simulation of a geomagnetic field reversal. *Nature*, **377**: 203–209.

Glatzmaier, G.A., and Roberts, P.H., 1997. Simulating the geodynamo. *Contemporary Physics*, **38**: 269–288.

Glatzmaier, G.A., Coe, R.S., Hongre, L., and Roberts, P.H., 1999. The role of the Earth's mantle in controlling the frequency of geomagnetic reversals. *Nature*, **401**: 885–890.

Hollerbach, R., 1996. On the theory of the geodynamo. *Physics of the Earth and Planetary Interiors*, **98**: 163–185.

Jones, C.A., Longbottom, A., and Hollerbach, R., 1995. A self-consistent convection driven geodynamo model, using a mean field approximation. *Physics of the Earth and Planetary Interiors*, **92**: 119–141.

Kageyama, A., Ochi, M., and Sato, T., 1999. Flip-flop transitions of the magnetic intensity and polarity reversals in the magnetohydrodynamic dynamo. *Physics Review Letters*, **82**: 5409–5412.

Kageyama, A., Sato, T., Watanabe, K., Horiuchi, R., Hayashi, T. *et al.,* 1995. Computer simulation of a magnetohydrodynamic dynamo. II. *Physics of Plasmas*, **2**: 1421–1431.

Kono, M., and Roberts, P.H., 2002. Recent geodynamo simulations and observations of the geomagnetic field. *Review of Geophysics*, **40**: 41–53.

Kutzner, C., and Christensen, U.R., 2002. From stable dipolar towards reversing numerical dynamos. *Physics of the Earth and Planetary Interiors*, **131**: 29–45.

Roberts, P.H., and Glatzmaier, G.A., 2000. Geodynamo theory and simulations. *Reviews of Modern Physics*, **72**: 1081–1123.

Sakuraba, A., and Kono, M., 1999. Effect of the inner core on the numerical solution of the magnetohydrodynamic dynamo. *Physics of the Earth and Planetary Interiors*, **111**: 105–121.

Sarson, G.R., and Jones, C.A., 1999. A convection driven dynamo reversal model. *Physics of the Earth and Planetary Interiors*, **111**: 3–20.

Zhang, K., and Busse, F.H., 1988. Finite amplitude convection and magnetic field generation in a rotating spherical shell. *Geophysical and Astrophysical Fluid Dynamics*, **41**: 33–53.

Cross-references

Core Convection
Core Turbulence
Core Viscosity
Core–Mantle Boundary Topography, Implications for Dynamics
Core–Mantle Coupling, Electromagnetic
Core–Mantle Coupling, Thermal
Core–Mantle Coupling, Topographic
Dynamo, Solar
Geodynamo
Geomagnetic Dipole Field
Harmonics, Spherical
Inner Core Rotation
Inner Core Seismic Velocities
Inner Core Tangent Cylinder
Magnetohydrodynamics
Reversals, Theory
Thermal Wind
Westward Drift

GEODYNAMO, SYMMETRY PROPERTIES

The behavior of any physical system is determined in part by its symmetry properties. For the geodynamo this means the geometry of a spinning sphere and the symmetry properties of the equations of magnetohydrodynamics. Solutions have symmetry that is the same as, or lower than, the symmetry of the governing equations and boundary conditions. By "symmetry" here we mean a transformation T that takes the system into itself. Given one solution with lower symmetry, we can construct a second solution by applying the transformation T to it. Solutions with different symmetry can evolve independently and are said to be *separable*. If the governing equations are linear separable solutions are also linearly independent: they may be combined to form a more general solution. If the governing equations are nonlinear they may not be combined or coexist but they remain separable. The full *geodynamo* (*q.v.*) problem is nonlinear and separable solutions exist; fluid velocities and magnetic fields with the same symmetry are linearly independent solutions of the linear *kinematic dynamo* (*q.v.*) problem.

Symmetry considerations are important for both theory and observation. For example, solutions with high symmetry are easier to compute than those with lower symmetry and are often chosen for that reason. Time-dependent behavior of nonlinear systems (geomagnetic reversals for example) may be analyzed in terms of one separable solution becoming unstable to one with different symmetry ("symmetry breaking"). Observational applications include detection of symmetries in the geomagnetic field. The axial dipole field has very high symmetry but is not a separable solution of the geodynamo; it does, however, belong to a separable solution with a particular symmetry about the equator. Paleomagnetic data rarely have sufficient global coverage to allow a proper assessment of the spatial pattern of the geomagnetic field, but they can sometimes be used to discriminate between separable solutions with different symmetries.

The sphere is symmetric under any rotation about its centre while rotation is symmetric under any rotation about the spin axis. The symmetries of the spinning sphere are therefore any rotation about the spin axis and reflection in the equatorial plane (Figure G15). This conflict of spherical and cylindrical geometry lies at the heart of many of the properties of rotating convection and the geodynamo. The equations of *magnetohydrodynamics* (*q.v.*) are also invariant under rotation. They are invariant under change of sign of magnetic field B (but not other dependent variables) because the induction equation is linear in B and the magnetic force and ohmic heating are quadratic in B. They are also invariant under time translation.

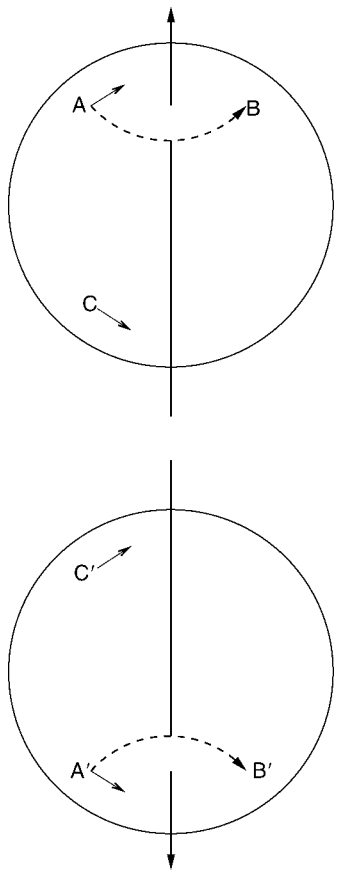

Figure G15 Reflection of a rotating sphere in a plane parallel to the equator. A′ , B′ are the reflections of the points A, B. The reflected sphere turns in the same direction as the original sphere. A vector is equatorial-symmetric (E^S) if its value at C′ appears as a reflection as shown: it is E^A if it appears with a change of sign.

The group of symmetry operations is Abelian because of the infinite number of allowed rotations about the spin axis and time translations. The full set of symmetry operations is found by constructing the group table and using the closure property. The group table, including rotation of π about the spin axis but no higher rotations, is shown in Table G6. Note the additional symmetry operations O; these are combinations of reflection in the equatorial plane and rotation about the spin axis; they amount to reflection through the origin. Note also the subgroups formed by (I,i) and (I,i,E^S,E^A). These are fundamental to some analyses of paleomagnetic data. Arbitrary time translation can be applied to any symmetry to produce steady solutions that are invariant under translation, drifting solutions that are steady in a corotating frame, more complicated time-periodic solutions that may vascillate or have reversing magnetic fields, and solutions that change continually and are sometimes loosely called "chaotic."

A word is needed about the behavior of vectors under reflection. A vector is usually defined by its transformation law under rotation. An axial or pseudovector (or tensor) changes sign on reflection whereas a polar or true vector (or tensor) does not. A true scalar is invariant under reflection, a pseudoscalar changes sign. Examples of true vectors are fluid velocity and electric current. Examples of axial vectors are angular velocity and magnetic field. The cross product changes sign under reflection (to see this consider the simple case of the cross product of two polar vectors); the curl also changes sign under reflection. Vectors v satisfying $\nabla \cdot v = 0$ are often represented in terms of their toroidal and poloidal parts:

http://www.springer.com/978-1-4020-3992-8

Encyclopedia of Geomagnetism and Paleomagnetism
Gubbins, D.; Herrero-Bervera, E. (Eds.)
2007, XXVI, 1054 p. 718 illus., 50 illus. in color.,
Hardcover
ISBN: 978-1-4020-3992-8